2008 IEEE/RSJ International Conference on Intelligent Robots and Systems
Acropolis Convention Center
Nice, France, Sept, 22-26, 2008

Impedance Control for Variable Stiffness Mechanisms with Nonlinear Joint Coupling

Thomas Wimböck*, Christian Ott†, Alin Albu-Schäffer*, Andreas Kugi‡ and Gerd Hirzinger*
*Institute of Robotics and Mechatronics, German Aerospace Center (DLR), Germany, Email: thomas.wimboeck@dlr.de
†Department of Mechano-Informatics, University of Tokyo, Japan
‡Automation & Control Institute (ACIN), TU Vienna, Austria

Abstract— **The current discussion on physical human robot interaction and the related safety aspects, but also the interest of neuro-scientists to validate their hypotheses on human motor skills with bio-mimetic robots, led to a recent revival of tendon-driven robots. In this paper, the modeling of tendon-driven elastic systems with nonlinear couplings is recapitulated. A control law is developed that takes the desired joint position and stiffness as input. Therefore, desired motor positions are determined that are commanded to an impedance controller. We give a physical interpretation of the controller. More importantly, a static decoupling of the joint motion and the stiffness variation is given. The combination of active (controller) and passive (mechanical) stiffness is investigated. The controller stiffness is designed according to the desired overall stiffness. A damping design of the impedance controller is included in these considerations. The controller performance is evaluated in simulation.**

I. Introduction

The growing interest in physical human robot interaction and the interest of neuro-scientists to validate their hypotheses on human motor skills with bio-mimetic robots motivate the design of highly anthropomorphic robots. Herein, the design of a robot hand is a great challenge, since it requires a large number of degrees of freedom (DOF) distributed on small space. In the DLR Hand II [1] 13 active DOF were realized by motors that are completely integrated within the hand, so that it can be mounted in a modular way to a robot wrist. The drawback of this design is that the robot hand became about 1.5 times larger than the human one. The relocation of the motors in the forearm via tendons is chosen for the novel DLR hand arm system [2] (cf. Fig. 1) enabling the realization of 19 antagonistic DOF, hence 38 motors, while achieving a human-like size. The implementation of the mechanical functionality required an asymmetric tendon routing with nonlinear couplings. The goal of this paper is to derive a control law for regulating the joint position and stiffness for this class of mechanisms.

Tahara et al. [3] study a dual-finger model with synergistic actuation of antagonist muscles. Based on Hill's model for the human muscle, a sensory-motor control rule for a planar robot realizing a stable dual-finger grasp of a rectangular object is presented. The object posture and the internal forces are controlled independently. In [4] the static model of a tendon-driven robot hand is presented by Bicchi and Prattichizzo and a constraint optimization is given.

Kobayashi and Ozawa [5] present an adaptive neural network control for tendon-driven robotic mechanisms with elastic tendons. An adaptive tracking controller is derived and its stability is proven for linear and nonlinear tendon elasticity. Global asymptotic tracking was proven for the case of linear elastic tendons. The desired motor positions are calculated from the implicit tendon force equation. This equation includes an estimate of the link-side dynamics and a link-side friction compensation term that are both mapped by the pseudoinverse of the tendon coupling matrix. Many aspects are treated in this work in order to develop an impedance controller for a quite general class of tendon systems. Some questions, however, like the selection of the appropriate metric for the pseudoinverse of the coupling matrix or the design and structure of the bias forces are not treated. Furthermore, there is no physical interpretation of the control law.

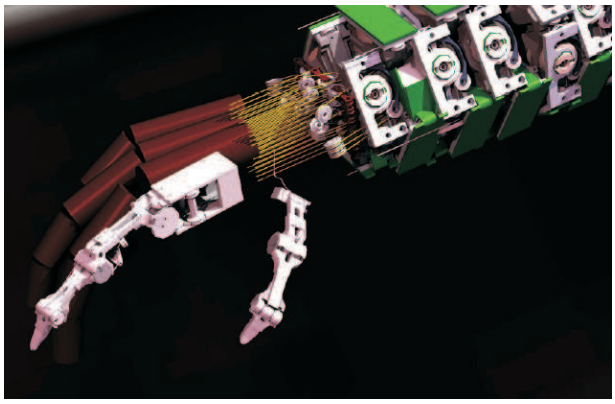

Fig. 1. CAD drawing of the DLR hand arm system [2].

In [6] Palli et al. studied the feedback linearization of uncoupled joints that are each driven antagonistically. Furthermore, an adaptive motor level PD controller was presented in [7] for a single antagonistic joint that was verified by means of experiments.

In the past, passivity-based impedance controllers for flexible joint robots were presented by Ott and Albu-Schäffer [8], [9]. In this framework, the emphasis was to derive controllers from potential functions and to develop control laws that realize a predefined stiffness characteristics in the joints by means of control. Thereby, a gravity compensation strategy for flexible joint manipulators and a consequent

damping and effective stiffness[1] design were presented for serial kinematic chains. Furthermore, the framework provides an intuitive physical interpretation. In contrast to the work of Ott and Albu-Schäffer, the control of a tendon-driven robotic mechanism requires several extensions. The consideration of linear joint elasticity has to be extended to nonlinear tendon elasticity, enabling to define a variable mechanical joint stiffness [2], [10]. The calculation of the effective stiffness must be modified to cope with coordinate transformations between tendon and joint space and the linearization of the nonlinear tendon stiffness. The *pulling constraints* of the tendons have to be ensured, i. e., via tendons one can only pull and not push the joints. Due to the parallel kinematics it is also necessary to handle coordinates that are related to internal motion.

The main contributions of this paper are as follows. Firstly, the calculation of the desired tendon positions giving the desired joint positions and stiffness in the case of nonlinear coupling and exponential tendon stiffness is presented. This derivation does not require the use of the pseudoinverse of the coupling matrix. Secondly, a new multi-DOF impedance control law is proposed including an effective joint stiffness design together with a damping design. This design allows to prescribe an effective joint stiffness by utilizing both the passive mechanical stiffness and the active controller stiffness. E.g., the diagonal terms of the mechanical stiffness of a hyperboloid joint driven by four tendons [2] cannot be set independently.

In this paper, first the modeling of tendon-driven elastic systems with nonlinear coupling is recapitulated. In Section III the inverse problem is addressed, which requires to solve for motor positions given the desired joint position and stiffness. These motor positions are used in a control law described in Section IV. The presented algorithms are evaluated by simulating an anthropomorphic robot finger in Section V.

II. Model of a multi DOF tendon-driven variable stiffness robot

In Fig. 2, a simple tendon-network consisting of two joints and four tendons connected by nonlinear springs is shown. In Table I, the variables to describe the equations of motion of a multi DOF tendon-driven variable stiffness robot are given. The tendon inverse kinematics $\boldsymbol{h}_q(\boldsymbol{q})$ gives the tendon positions as a function of the joint angles $\boldsymbol{q}$. The function $\boldsymbol{h}_q(\boldsymbol{q})$ can be used to derive a differential map $\boldsymbol{P}(\boldsymbol{q})$:

$$\boldsymbol{P}(\boldsymbol{q}) \quad = \quad \left(\frac{\partial \boldsymbol{h}_q(\boldsymbol{q})}{\partial \boldsymbol{q}}\right)^T. \tag{1}$$

In the literature this map is also known as *coupling matrix* [11]. Note that in contrast to the Jacobian matrix of a serial kinematic chain, the transposed coupling matrix maps from joint to tendon velocities

$$\dot{\boldsymbol{h}}_q \quad = \quad \boldsymbol{P}^T(\boldsymbol{q})\dot{\boldsymbol{q}} \tag{2}$$

[1]The effective stiffness expresses the amount of local displacement of a generalized coordinate w.r.t. a corresponding generalized force. Thus, all contributions to the effective stiffness are taken into account.

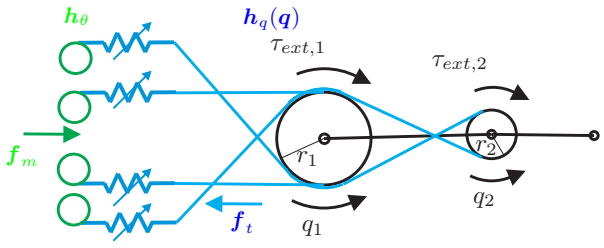

Fig. 2. Simple example of a tendon network with two joints and four tendons connected by nonlinear springs.

$\boldsymbol{q}$	$\in$	$\mathbb{R}^n$	n Joint positions
$\boldsymbol{\theta}$	$\in$	$\mathbb{R}^m$	m Motor positions
$\boldsymbol{h}_q(\boldsymbol{q})$	$\in$	$\mathbb{R}^m$	m Tendon length changes w. r. t. joints
$\boldsymbol{h}_\theta(\boldsymbol{\theta})$	$\in$	$\mathbb{R}^m$	m Tendon length changes w. r. t. motor
$\boldsymbol{M}(\boldsymbol{q})$	$\in$	$\mathbb{R}^{n\times n}$	Positive definite (p. d.) inertia matrix
$\boldsymbol{M}_h$	$\in$	$\mathbb{R}^{m\times m}$	P. d. effective tendon inertia matrix including motor inertia
$\boldsymbol{C}(\boldsymbol{q},\dot{\boldsymbol{q}})\dot{\boldsymbol{q}}$	$\in$	$\mathbb{R}^n$	Link-side centrifugal and Coriolis terms
$\boldsymbol{g}(\boldsymbol{q})$	$\in$	$\mathbb{R}^n$	Link-side gravity vector
$\boldsymbol{\tau}_{ext}$	$\in$	$\mathbb{R}^n$	External torque
$\boldsymbol{f}_m$	$\in$	$\mathbb{R}^m$	Tendon motor forces (control input)
$\boldsymbol{f}_t$	$\in$	$\mathbb{R}^m$	Tendon forces
$\boldsymbol{f}_{f,\theta}$	$\in$	$\mathbb{R}^m$	Motor friction forces
$\boldsymbol{\tau}_f$	$\in$	$\mathbb{R}^n$	Joint friction torque (viscous)

TABLE I
Definition of variables.

and the tendon forces are related to the joint torques by

$$\boldsymbol{\tau}_q \quad = \quad \boldsymbol{P}(\boldsymbol{q})\boldsymbol{f}_t. \tag{3}$$

For a well-designed mechanism the coupling matrix $\boldsymbol{P}(\boldsymbol{q})$ has full row rank over the whole configuration space [12].

Using the coupling matrix $\boldsymbol{P}(\boldsymbol{q})$ it is straightforward to formulate the equations of motion [11]:

$$\boldsymbol{M}(\boldsymbol{q})\ddot{\boldsymbol{q}} + \boldsymbol{C}(\boldsymbol{q},\dot{\boldsymbol{q}})\dot{\boldsymbol{q}} + \boldsymbol{\tau}_f + \boldsymbol{g}(\boldsymbol{q}) \quad = \quad \boldsymbol{P}(\boldsymbol{q})\boldsymbol{f}_t + \boldsymbol{\tau}_{ext} \tag{4}$$

$$\boldsymbol{M}_h\ddot{\boldsymbol{h}}_\theta + \boldsymbol{f}_{f,\theta} + \boldsymbol{f}_t \quad = \quad \boldsymbol{f}_m\ . \tag{5}$$

These equations are only valid as long as the inequality constraint of pulling tendons is fulfilled, i. e.,

$$\boldsymbol{f}_{t,i} > 0, \quad \forall i = 1,\ldots,m. \tag{6}$$

We assume in the following that the input values to the proposed controller can be chosen such that this constraint is fulfilled at any time if the resulting pre-tension is sufficiently high.

The tendon force can be modeled as a function of the displacement of the motor and the joint tendon length changes. A suitable function resulting in a progressive tendon stiffness can be described for tendon i by the exponential function

$$\boldsymbol{f}_{t,i}(h_{\theta_i}, h_{q_i}) = k_{t_i}(e^{\gamma_i \Delta h_i} - 1), \quad \forall i = 1,\ldots,m, \tag{7}$$

with the elongation of the tendon given by $\Delta h_i = h_{\theta_i} - h_{q_i}$, and the parameters $k_{t_i} > 0, \gamma_i \in \mathbb{R}$. This means that a change in tendon length results in a modification of the tendon force as long as the pulling constraint (6) is fulfilled.

In Section III we use the fact that the tendon stiffness of such a characteristics an affine function of the tendon force.

Note that henceforth the desired value of a variable will be denoted by the additional index d.

III. Inverse solution

From an application point of view, it is desirable to specify the link-side position $\boldsymbol{q}_d \in \mathbb{R}^n$ and the symmetric positive definite (p.d.) mechanical joint stiffness $\boldsymbol{S}_d \in \mathbb{R}^{n\times n}$. However, it is easy to show that a control law based on link-side position measurements is not passive. A method is to solve the inverse problem that maps $\boldsymbol{q}_d$ and $\boldsymbol{S}_d$ to desired motor positions $\boldsymbol{h}_{\theta,d}$ [7], [13]. The first set of equations is given by the steady-state of the equations of motion of the link-side (4) while setting the steady-state values as the desired ones:

$$\boldsymbol{g}(\boldsymbol{q}_d) - \boldsymbol{P}(\boldsymbol{q}_d)\boldsymbol{f}_{t,d} = \boldsymbol{\tau}_{ext}(\boldsymbol{h}_{\theta,d}, \boldsymbol{q}_d), \tag{8}$$

with $\boldsymbol{f}_{t,d} = \boldsymbol{f}_t(\boldsymbol{h}_{\theta,d}, \boldsymbol{h}_q(\boldsymbol{q}_d))$ the vector containing the desired tendon forces. In order to specify the mechanical stiffness $\boldsymbol{S}_d(\boldsymbol{h}_{\theta,d}, \boldsymbol{q}_d)$ for a given $\boldsymbol{q}_d$ we determine the local behavior of $\boldsymbol{q}$ w.r.t. to an external torque $\tau_{ext}(\boldsymbol{h}_{\theta,d}, \boldsymbol{q})$ for a fixed desired motor position $\boldsymbol{h}_{\theta,d}$, i.e.

$$\boldsymbol{S}_d(\boldsymbol{h}_{\theta,d}, \boldsymbol{q}_d) = \left(\frac{\partial \boldsymbol{\tau}_{ext}(\boldsymbol{h}_{\theta,d}, \boldsymbol{q})}{\partial \boldsymbol{q}}\right)\Bigg|_{\boldsymbol{q}=\boldsymbol{q}_d}. \tag{9}$$

Due to the symmetry of the stiffness matrix *at most* $(n+1)n/2$ independent nonlinear equations can be derived. Together with the n equations from (8) required to impose $\boldsymbol{q}_d$ and the m equations from the tendon force model (7), at most $(n+3)n/2+m$ equations are obtained to solve for the $2m$ unknown variables $\boldsymbol{h}_{\theta,d}$ and $\boldsymbol{f}_{t,d}$. In the special case of uncoupled joints, it is sufficient to consider only the diagonal matrix elements of $\boldsymbol{S}_d$ leading to $2n+m$ equations. Other special cases like symmetrically coupled tendon networks are described in [12]. Inserting $\boldsymbol{\tau}_{ext}(\boldsymbol{h}_{\theta,d}, \boldsymbol{q})$ from (8) into the joint stiffness (9) and using the exponential tendon force characteristics (7) gives

$$\begin{aligned}\boldsymbol{S}_d \;=\; & \frac{\partial \boldsymbol{g}(\boldsymbol{q}_d)}{\partial \boldsymbol{q}_d} - \frac{\partial \boldsymbol{P}(\boldsymbol{q}_d)}{\partial \boldsymbol{q}_d}\boldsymbol{f}_{t,d} \\ & + \boldsymbol{P}(\boldsymbol{q}_d)\boldsymbol{\Gamma}\mathrm{diag}\{\boldsymbol{f}_{t,d} + \boldsymbol{k}_t\}\boldsymbol{P}^T(\boldsymbol{q}_d),\end{aligned} \tag{10}$$

with the matrix $\boldsymbol{\Gamma} \in \mathbb{R}^{n\times n} = \mathrm{diag}\{\gamma_1, \ldots, \gamma_n\}$, the vector $\boldsymbol{k}_t = (k_{t_1}, \ldots, k_{t_n})^T$ containing the tendon force parameters, and the tendon stiffness $\frac{\partial \boldsymbol{f}_t(\boldsymbol{h}_{\theta,d}, \boldsymbol{h}_q)}{\partial \boldsymbol{h}_q}\Big|_{\boldsymbol{q}=\boldsymbol{q}_d} = -\boldsymbol{\Gamma}\mathrm{diag}\{\boldsymbol{f}_{t,d} + \boldsymbol{k}_t\}$. It is important to mention that the term $\frac{\partial \boldsymbol{h}_{\theta,d}}{\partial \boldsymbol{q}} = \boldsymbol{0}$, because $\boldsymbol{h}_{\theta,d}$ is the constant setpoint for the underlying impedance controller presented in the next section. Note that the term $\frac{\partial \boldsymbol{h}_\theta}{\partial \boldsymbol{q}} \neq \boldsymbol{0}$ is included in the derivation of the effective stiffness in the following section.

In [12] this inverse problem is solved for tendon-driven mechanisms with an exponential characteristics of the tendon stiffness as defined in equation (7). However, in [12] the coupling matrix $\boldsymbol{P}(\boldsymbol{q})$ is assumed to be independent of the link positions, and furthermore, the gravity term is neglected. Based on this stiffness matrix a stiffness vector is derived. Combined with the steady-state equation (8), the tendon forces are calculated by linear programming involving the pseudoinverse and the nullspace projection of the coupling matrix. With a proper choice of the tendon force model the desired tendon positions $\boldsymbol{h}_{\theta,d}$ can then be determined uniquely.

In the following, we propose a way to determine $\boldsymbol{h}_{\theta,d}$ for a tendon-network with nonlinear elasticity and nonlinear tendon routing. Furthermore, link gravity is included in our inverse solution. Notice that, if the problem is well defined, i.e. one specifies $m-n$ stiffness components, there is no need for pseudoinversion[2]. First, the operation

$$\begin{aligned}\mathrm{sv}\{\boldsymbol{S}\} &: \mathbb{R}^{n\times n} \to \mathbb{R}^{\frac{(n+1)n}{2}} \\ \mathrm{sv}\{\boldsymbol{S}\} &= s_{i(i-1)/2+j} = S_{ij};\; i,j = 1,2,\ldots,n;\; i \geq j\end{aligned} \tag{11}$$

that generates the stiffness vector $\boldsymbol{s}$ representing uniquely a stiffness matrix is defined. Since the stiffness equation (10) is affine in the tendon force $\boldsymbol{f}_{t,d}$ we rewrite the equation in the stiffness vectorized form

$$\mathrm{sv}\{\boldsymbol{S}_d - \boldsymbol{S}_g(\boldsymbol{q}_d) - \boldsymbol{S}_k(\boldsymbol{q}_d)\} = \boldsymbol{S}_t(\boldsymbol{q}_d)\boldsymbol{f}_{t,d}, \tag{12}$$

with the gravity induced stiffness $\boldsymbol{S}_g(\boldsymbol{q}_d) = \frac{\partial \boldsymbol{g}(\boldsymbol{q}_d)}{\partial \boldsymbol{q}_d}$. The term $\boldsymbol{S}_k(\boldsymbol{q}_d) = \boldsymbol{P}(\boldsymbol{q}_d)\boldsymbol{\Gamma}\mathrm{diag}\{\boldsymbol{k}_t\}\boldsymbol{P}^T(\boldsymbol{q}_d)$ is obtained by setting $\Delta\boldsymbol{h} = \boldsymbol{0}$ and consequently $\boldsymbol{f}_{t,d} = \boldsymbol{0}$ and can be seen as the minimal stiffness[3] fulfilling the pulling constraint (6) for $\boldsymbol{S}_g(\boldsymbol{q}_d) = \boldsymbol{0}$. The re-parametrization of the tendon induced stiffness $\boldsymbol{S}_t(\boldsymbol{q}_d) \in \mathbb{R}^{\frac{(n+1)n}{2}\times n}$ can be expressed as

$$\boldsymbol{S}_t(\boldsymbol{q}_d)\boldsymbol{f}_{t,d} = \mathrm{sv}\{-\frac{\partial \boldsymbol{P}(\boldsymbol{q}_d)}{\partial \boldsymbol{q}_d}\boldsymbol{f}_{t,d} + \boldsymbol{P}(\boldsymbol{q}_d)\boldsymbol{\Gamma}\mathrm{diag}\{\boldsymbol{f}_{t,d}\}\boldsymbol{P}^T(\boldsymbol{q}_d)\}. \tag{13}$$

In order to solve for the tendon force, these equations are stacked together with the steady-state solution (8). It is important to set the external torque $\boldsymbol{\tau}_{ext}$ to zero here. If used in this equation, every external torque would be compensated so that the joint behaves as force and not impedance controlled. This way we obtain

$$\begin{pmatrix} \boldsymbol{g}(\boldsymbol{q}_d) \\ \mathrm{sv}\{\boldsymbol{S}_d - \boldsymbol{S}_g(\boldsymbol{q}_d) - \boldsymbol{S}_k(\boldsymbol{q}_d)\} \end{pmatrix} = \underbrace{\begin{bmatrix} \boldsymbol{P}(\boldsymbol{q}_d) \\ \boldsymbol{S}_t(\boldsymbol{q}_d) \end{bmatrix}}_{\boldsymbol{Q}^T(\boldsymbol{q}_d)} \boldsymbol{f}_{t,d}. \tag{14}$$

The desired tendon force can be calculated if $\boldsymbol{Q}^{-T}(\boldsymbol{q}_d)$ exists

$$\boldsymbol{f}_{t,d} = \boldsymbol{Q}^{-T}(\boldsymbol{q}_d)\begin{pmatrix} \boldsymbol{g}(\boldsymbol{q}_d) \\ \mathrm{sv}\{\boldsymbol{S}_d - \boldsymbol{S}_g(\boldsymbol{q}_d) - \boldsymbol{S}_k(\boldsymbol{q}_d)\} \end{pmatrix}. \tag{15}$$

On the existence of $\boldsymbol{Q}^{-T}(\boldsymbol{q}_d)$ and joint stiffness adjustability: In order to obtain an invertible matrix, $\boldsymbol{Q}(\boldsymbol{q}_d)$ has to have rank $\frac{(n+3)n}{2}$. This implies that the number of tendons must be at least $m = \frac{(n+3)n}{2}$. In [12] such a mechanism is called to be *minimal joint stiffness adjustable*. Note that due to the pulling constraint (6) the elements of the stiffness matrix cannot be chosen arbitrarily.

[2]Methods similar to [14] can be used for the best approximation if $\boldsymbol{S}_d$ is fully specified, but $m < \frac{n(n+3)}{2}$.

[3]This minimal stiffness is due to the property of the exponential function since its derivative is only zero at $-\infty$.

In mechanisms that are not joint stiffness adjustable, a selection of entries in $\boldsymbol{S}_d$ has to be made s. t. $\boldsymbol{Q}(\boldsymbol{q}_d)$ has full rank. In many cases the most relevant elements are the diagonal stiffness components. For example, given a tendon-controllable asymmetric network with 4 joints and 8 tendons, four rows in $\boldsymbol{Q}(\boldsymbol{q}_d)$ remain for the stiffness adjustment. The most intuitive choice is to select the diagonal elements if they can be set independently by the mechanism. Since the joint stiffness coupling terms cannot be assigned they will then result as a function of the joint configuration $\boldsymbol{q}_d$ and the diagonal stiffness components.

The desired tendon force (15) is finally folded back into equation (7) to solve for the desired motor positions

$$h_{\theta_i,d} \quad = \quad h_{q_i}(\boldsymbol{q}_d) + \frac{1}{\gamma_i}\ln\{\frac{f_{t,d_i}}{k_{t_i}} + 1\}. \tag{16}$$

This equation is very similar to the well-known formula for flexible joints [15].

IV. Control Strategy

A. Controller structure

The goal of this section is to derive an impedance controller. Figure 3 depicts a simple control structure. The inverse calculation of Section III produces the desired motor positions and the desired tendon forces. The motor controller realizes the impedance behavior with the tendon forces $\boldsymbol{f}_m$ as control inputs. A more complex control structure using

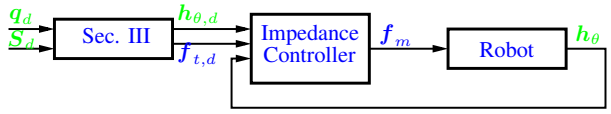

Fig. 3. Block diagram of the simple control structure.

the measurements of the tendon force is presented in Fig. 4. The output of the impedance controller is now the input to an underlying force controller that reshapes the motor inertia.

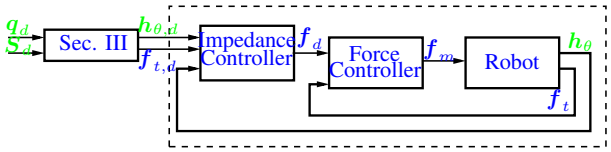

Fig. 4. Block diagram of the control structure with an inner force control loop.

B. Reshaping the motor inertia

In [16], the local feedback of the joint torque is used to generate a low-level controller that can be interpreted as a reshaping of the motor inertia. This physically intuitive control law can be applied in a similar fashion to a tendon driven system. With $\boldsymbol{M}_{h,d} \in \mathbb{R}^{m\times m}$ as the desired diagonal motor inertia matrix the control law follows as

$$\boldsymbol{f}_m = \boldsymbol{M}_h\boldsymbol{M}_{h,d}^{-1}\boldsymbol{f}_d + (\mathbf{I} - \boldsymbol{M}_h\boldsymbol{M}_{h,d}^{-1})\boldsymbol{f}_t + \boldsymbol{f}_{f,\theta}. \tag{17}$$

The equation of the motor side dynamics (5) becomes

$$\boldsymbol{M}_{h,d}\ddot{\boldsymbol{h}}_\theta + \boldsymbol{f}_t = \boldsymbol{f}_d. \tag{18}$$

The vector $\boldsymbol{f}_d$ is the new control input for the impedance controller of the outer control loop. Note that the motor friction $\boldsymbol{f}_{f,\theta}$ is compensated here.

C. Tendon Control

The outer control loop that realizes the motor level impedance control can be given as

$$\boldsymbol{f}_d = -\boldsymbol{K}_h\boldsymbol{e}_h - \boldsymbol{D}_h\dot{\boldsymbol{e}}_h + \boldsymbol{f}_{t,d} + \boldsymbol{M}_{h,d}\ddot{\boldsymbol{h}}_{\theta,d}, \tag{19}$$

with $\boldsymbol{K}_h, \boldsymbol{D}_h \in \mathbb{R}^{m\times m}$ the controlled stiffness and damping matrices of the controller and $\boldsymbol{e}_h = \boldsymbol{h}_\theta - \boldsymbol{h}_{\theta,d}$. The feed-forward term $\boldsymbol{M}_{h,d}\ddot{\boldsymbol{h}}_{\theta,d}$ is added for completeness; in practice this term is not applied due to its computational complexity. One intuitive choice of parametrization of the controlled stiffness and damping is to design a controller for each tendon or motor, respectively. This has the advantage that the control design is easy since the tendon coupling is ignored and $\boldsymbol{K}_h, \boldsymbol{D}_h$ are diagonal. The controlled stiffness is serial to the adjusted mechanical one. Thus, the effective stiffness at the link can be reduced by reducing either the controlled or the mechanical stiffness components. By controlling in motor coordinates, the position and stiffness are coupled by $\boldsymbol{K}_h$. When using a diagonal controlled stiffness we are quite limited in reducing the active stiffness, since the motors have to hold the desired tendon position in which the pre-tension is ensured. With low active stiffness it cannot be guaranteed that the tendon force can be kept within the pulling constraint.

D. Static Decoupling

In [13] a change of coordinates is performed to relate the motor position errors to errors due to the joint motion and the stiffness adjustment for a single antagonistic joint[4]. In order to extend this idea to a multi DOF mechanism the coupling matrix has to be investigated. In quasi-static condition, the change in tendon length at the motors equals the tendon displacement due to joint motion plus the tendon motion that is related to stiffness adjustment. In equation (14) the tendon forces are mapped to a stacked vector containing the joint torque due to gravity and the stiffness vector at the desired position. In a similar fashion we can derive the locally valid relationship starting with the steady-state and the stiffness equation of the mechanism (8) and (10) using the joint angles $\boldsymbol{q}$ and stiffness vector[5] $\boldsymbol{s} = \mathrm{sv}\{\boldsymbol{S}\}$ instead of the desired ones, i. e.

$$\boldsymbol{f}_{\bar{q}\bar{s}} = \boldsymbol{Q}^T(\boldsymbol{q})\boldsymbol{f}_d, \text{with} \tag{20}$$

$$\boldsymbol{Q}^T(\boldsymbol{q}) = \begin{bmatrix} \boldsymbol{P}(\boldsymbol{q}) \\ \boldsymbol{S}_t(\boldsymbol{q}) \end{bmatrix} \quad \text{and} \quad \boldsymbol{f}_{\bar{q}\bar{s}} = \begin{pmatrix} \boldsymbol{\tau}_q \\ \boldsymbol{s} \end{pmatrix}. \tag{21}$$

[4]The coupling matrix of a single antagonistic joint with radius r is $\boldsymbol{P} = [r, -r]$.

[5]The actual mechanical stiffness $\boldsymbol{S}$ is computed using equation (10) based on the current values and not the desired ones.

Using the principle of virtual work $\dot{\boldsymbol{e}}_h^T \boldsymbol{f}_d = \dot{\boldsymbol{e}}_{\bar{qs}}^T \boldsymbol{f}_{\bar{qs}}$ the relationship

$$\begin{aligned} \dot{\boldsymbol{e}}_h &= \boldsymbol{Q}(\boldsymbol{q})\dot{\boldsymbol{e}}_{\bar{qs}} \quad (22) \\ \delta\boldsymbol{e}_h &= \boldsymbol{Q}(\boldsymbol{q})\delta\boldsymbol{e}_{\bar{qs}} \quad (23) \end{aligned}$$

is obtained. Thus, the corresponding control law can be written as, cf. (19),

$$\begin{aligned} \boldsymbol{f}_d = &- \underbrace{\boldsymbol{Q}^{-T}\boldsymbol{K}_{\bar{qs}}\boldsymbol{Q}^{-1}}_{\boldsymbol{K}^h_{\bar{qs}}(\boldsymbol{q})}\boldsymbol{e}_h - \underbrace{\boldsymbol{Q}^{-T}\boldsymbol{D}_{\bar{qs}}\boldsymbol{Q}^{-1}}_{\boldsymbol{D}^h_{\bar{qs}}(\boldsymbol{q})}\dot{\boldsymbol{e}}_h \\ &+ \boldsymbol{f}_{t,d} + \boldsymbol{M}_{h,d}\ddot{\boldsymbol{h}}_{\theta,d}, \end{aligned} \quad (24)$$

with $\boldsymbol{K}_{\bar{qs}}, \boldsymbol{D}_{\bar{qs}} \in \mathbb{R}^{m\times m}$

$$\boldsymbol{K}_{\bar{qs}} = \begin{bmatrix} \boldsymbol{K}_q & \boldsymbol{0} \\ \boldsymbol{0} & \boldsymbol{K}_s \end{bmatrix} \quad \boldsymbol{D}_{\bar{qs}} = \begin{bmatrix} \boldsymbol{D}_q & \boldsymbol{0} \\ \boldsymbol{0} & \boldsymbol{D}_s \end{bmatrix} \quad (25)$$

the stiffness and damping matrices on task level. In this way it is possible to relate the stiffness components to the variables that were chosen by the generation of the joint torques and the stiffness vector $\boldsymbol{s}$. Inserting this control law in the closed-loop equations of the force controller (18) gives

$$\boldsymbol{M}_{h,d}\ddot{\boldsymbol{e}}_h + \boldsymbol{D}^h_{\bar{qs}}(\boldsymbol{q})\dot{\boldsymbol{e}}_h + \boldsymbol{K}^h_{\bar{qs}}(\boldsymbol{q})\boldsymbol{e}_h + \Delta\boldsymbol{f}_t = \boldsymbol{0}, \quad (26)$$

with the error in the tendon force $\Delta\boldsymbol{f}_t = \boldsymbol{f}_t - \boldsymbol{f}_{t,d}$.

Note that this method is closely related to the well-known *augmented Jacobian* method used for redundancy resolution [17]. Furthermore, this approach does not require an exponential characteristic of the tendon force. The matrix $\boldsymbol{Q}(\boldsymbol{q})$ could be also obtained in another way, e.g. by singular value decomposition of the coupling matrix. However, in this case it would not be possible to identify the coordinates related to the change in the tendon pretension as joint stiffness values.

E. Linearization of the Closed Loop Dynamics

In this section the closed loop dynamics of the whole tendon mechanism (4) and (26) are linearized. This model is then used to parameterize the controller stiffness $\boldsymbol{K}_q$ such that a locally valid effective stiffness can be derived. Rewritten in state space form with the state $\boldsymbol{x}^T = (\boldsymbol{q}, \dot{\boldsymbol{q}}, \boldsymbol{e}_h, \dot{\boldsymbol{e}}_h)$ while neglecting the joint friction, the equations become

$$\dot{\boldsymbol{x}} = \begin{pmatrix} \dot{\boldsymbol{q}} \\ \boldsymbol{M}^{-1}(\boldsymbol{q})[\boldsymbol{P}(\boldsymbol{q})\boldsymbol{f}_t(\boldsymbol{q}, \boldsymbol{e}_h + \boldsymbol{h}_{\theta,d}) - \\ \boldsymbol{C}(\boldsymbol{q}, \dot{\boldsymbol{q}})\dot{\boldsymbol{q}} - \boldsymbol{g}(\boldsymbol{q}) + \boldsymbol{\tau}_{ext}] \\ \dot{\boldsymbol{e}}_h \\ \boldsymbol{M}^{-1}_{h,d}[-\boldsymbol{K}^h_{\bar{qs}}(\boldsymbol{q})\boldsymbol{e}_h - \boldsymbol{D}^h_{\bar{qs}}(\boldsymbol{q})\dot{\boldsymbol{e}}_h - \\ \Delta\boldsymbol{f}_t(\boldsymbol{q}, \boldsymbol{e}_h + \boldsymbol{h}_{\theta,d})] \end{pmatrix}. \quad (27)$$

It is easy to show that $\boldsymbol{x}_d^T = (\boldsymbol{q}_d, \boldsymbol{0}, \boldsymbol{0}, \boldsymbol{0}), \boldsymbol{\tau}_{ext} = \boldsymbol{0}$ is an equilibrium of the closed loop system. The linearization around this equilibrium point can be calculated as

$$\Delta\dot{\boldsymbol{x}} = \begin{pmatrix} \Delta\dot{\boldsymbol{q}} \\ \boldsymbol{M}^{-1}(\boldsymbol{q}_d)[(\boldsymbol{L}_q(\boldsymbol{x}_d) - \boldsymbol{S}_g(\boldsymbol{q}_d))\Delta\boldsymbol{q} + \\ \boldsymbol{L}_e(\boldsymbol{x}_d)\Delta\boldsymbol{e}_h + \Delta\boldsymbol{\tau}_{ext}] \\ \Delta\dot{\boldsymbol{e}}_h \\ \boldsymbol{M}^{-1}_{h,d}[-\boldsymbol{\tau}_c - \boldsymbol{T}_q(\boldsymbol{x}_d)\Delta\boldsymbol{q} - \boldsymbol{T}_e(\boldsymbol{x}_d)\Delta\boldsymbol{e}_h] \end{pmatrix}, \quad (28)$$

with

$$\begin{aligned} \boldsymbol{\tau}_c &= \boldsymbol{K}^h_{\bar{qs}}(\boldsymbol{q}_d)\Delta\boldsymbol{e}_h + \boldsymbol{D}^h_{\bar{qs}}(\boldsymbol{q}_d)\Delta\dot{\boldsymbol{e}}_h \\ \boldsymbol{T}_q(\boldsymbol{x}_d) &= \left.\frac{\partial\boldsymbol{f}_t(\boldsymbol{q}, \boldsymbol{e}_h + \boldsymbol{h}_{\theta,d})}{\partial\boldsymbol{q}}\right|_{\boldsymbol{x}=\boldsymbol{x}_d} \\ \boldsymbol{T}_e(\boldsymbol{x}_d) &= \left.\frac{\partial\boldsymbol{f}_t(\boldsymbol{q}, \boldsymbol{e}_h + \boldsymbol{h}_{\theta,d})}{\partial\boldsymbol{e}_h}\right|_{\boldsymbol{x}=\boldsymbol{x}_d} \\ \boldsymbol{L}_q(\boldsymbol{x}_d) &= \left.\frac{\partial(\boldsymbol{P}(\boldsymbol{q})\boldsymbol{f}_t(\boldsymbol{q}, \boldsymbol{e}_h + \boldsymbol{h}_{\theta,d}))}{\partial\boldsymbol{q}}\right|_{\boldsymbol{x}=\boldsymbol{x}_d} \\ \boldsymbol{L}_e(\boldsymbol{x}_d) &= \left.\frac{\partial(\boldsymbol{P}(\boldsymbol{q})\boldsymbol{f}_t(\boldsymbol{q}, \boldsymbol{e}_h + \boldsymbol{h}_{\theta,d}))}{\partial\boldsymbol{e}_h}\right|_{\boldsymbol{x}=\boldsymbol{x}_d}, \end{aligned} \quad (29)$$

and the term $\boldsymbol{S}_g(\boldsymbol{q}_d) = \left.\frac{\partial\boldsymbol{g}(\boldsymbol{q})}{\partial\boldsymbol{q}}\right|_{\boldsymbol{x}=\boldsymbol{x}_d}$ describing a stiffness evoked by the gravity field of the mechanism acting parallel to the tendon stiffness on the joints. Note that the Coriolis terms disappear from the linearized equations since they are a quadratic function of the joint velocity $\dot{\boldsymbol{q}}$.

The partial derivatives in equation (29) can be rewritten using the definitions of $\Delta\boldsymbol{h}$ and $\boldsymbol{e}_h$. Defining $\boldsymbol{T}_f(\boldsymbol{x}_d) = \left.\frac{\partial\boldsymbol{f}_t(\boldsymbol{q}, \boldsymbol{e}_h + \boldsymbol{h}_{\theta,d})}{\partial(\Delta\boldsymbol{h})}\right|_{\boldsymbol{x}=\boldsymbol{x}_d} = \boldsymbol{T}_f^T(\boldsymbol{x}_d)$ we can write

$$\begin{aligned} \boldsymbol{T}_e(\boldsymbol{x}_d) &= \boldsymbol{T}_f(\boldsymbol{x}_d)\left.\frac{\partial(\Delta\boldsymbol{h})}{\partial\boldsymbol{h}_\theta}\frac{\partial\boldsymbol{h}_\theta}{\partial\boldsymbol{e}_h}\right|_{\boldsymbol{x}=\boldsymbol{x}_d} = \boldsymbol{T}_f(\boldsymbol{x}_d) \\ \boldsymbol{T}_q(\boldsymbol{x}_d) &= \boldsymbol{T}_f(\boldsymbol{x}_d)\left.\frac{\partial(\Delta\boldsymbol{h})}{\partial\boldsymbol{h}_q}\frac{\partial\boldsymbol{h}_q(\boldsymbol{q})}{\partial\boldsymbol{q}}\right|_{\boldsymbol{x}=\boldsymbol{x}_d} \\ &= -\boldsymbol{T}_f(\boldsymbol{x}_d)\boldsymbol{P}^T(\boldsymbol{q}_d), \end{aligned}$$

The term $\boldsymbol{L}_q(\boldsymbol{x}_d)$ contains the product of the coupling matrix and the nonlinear tendon force that are all a function of $\boldsymbol{q}$ leading to a complex expression given by

$$\boldsymbol{L}_q(\boldsymbol{x}_d) = -\boldsymbol{S}_p(\boldsymbol{x}_d) - \boldsymbol{P}(\boldsymbol{q}_d)\boldsymbol{T}_f(\boldsymbol{x}_d)\boldsymbol{P}^T(\boldsymbol{q}_d) \quad (30)$$

with $\boldsymbol{S}_p(\boldsymbol{x}_d) = -\left.\frac{\partial\boldsymbol{P}(\boldsymbol{q})}{\partial\boldsymbol{q}}\right|_{\boldsymbol{x}=\boldsymbol{x}_d}\boldsymbol{f}_t(\boldsymbol{q}_d, \boldsymbol{h}_{\theta,d})$ representing a stiffness due to the nonlinearity in the tendon routing that acts parallel to the tendon stiffness on the joints. The symmetry of $\boldsymbol{S}_p(\boldsymbol{x}_d)$ is shown in the appendix.

The behavior around the operating point can be now formulated as

$$\boldsymbol{M}\ddot{\boldsymbol{w}} + \boldsymbol{D}\dot{\boldsymbol{w}} + \boldsymbol{K}\boldsymbol{w} = \begin{pmatrix} \Delta\boldsymbol{\tau}_{ext} \\ \boldsymbol{0} \end{pmatrix}, \quad (31)$$

$$\boldsymbol{M} = \begin{bmatrix} \boldsymbol{M}_q(\boldsymbol{q}_d) & \boldsymbol{0} \\ \boldsymbol{0} & \boldsymbol{M}_{h,d} \end{bmatrix} \quad \boldsymbol{D} = \begin{bmatrix} \boldsymbol{0} & \boldsymbol{0} \\ \boldsymbol{0} & \boldsymbol{D}^h_{\bar{qs}} \end{bmatrix}$$

$$\boldsymbol{K} = \begin{bmatrix} \boldsymbol{S}_p + \boldsymbol{S}_g + \boldsymbol{P}\boldsymbol{T}_f\boldsymbol{P}^T & -\boldsymbol{P}\boldsymbol{T}_f \\ -\boldsymbol{T}_f\boldsymbol{P}^T & \boldsymbol{T}_f + \boldsymbol{K}^h_{\bar{qs}} \end{bmatrix},$$

with $\boldsymbol{w}^T = (\Delta\boldsymbol{q}, \Delta\boldsymbol{e}_h)$. Note that the matrix $\boldsymbol{K}$ is symmetric as long as the controller stiffness $\boldsymbol{K}_{\bar{qs}}$ is chosen symmetrically.

F. Effective Stiffness

The goal of an impedance controller is to give a mechanism the behavior of a desired impedance. In the past the intrinsic passive joint stiffness was used to calculate the controller stiffness, such that an effective, respectively

desired stiffness was obtained for serial kinematic chains [16]. In this work, we focus on the effective stiffness that can be determined for the steady-state and that is defined as $\Delta\boldsymbol{\tau}_{ext} = \boldsymbol{K}_{eq}\Delta\boldsymbol{q}$. In fact, it is not our goal to cancel out the natural mechanical joint stiffness by means of control since we want to use the mechanical properties to protect the robot from exerting large forces during impacts. We expect that in this way we can reduce the sampling time for the outer loop controller.

A standard technique to determine the effective stiffness is to transform the stiffness matrices in a common coordinate system and to identify the connectivity in terms of serial and parallel connections. In the stiffness matrix $\boldsymbol{K}$ of equation (31) we can identify the structure of two connected springs in series $\boldsymbol{K}_2, \boldsymbol{K}_q$ that are connected in parallel with $\boldsymbol{K}_1$[6] at the joints $\boldsymbol{q}$ (cf. Fig 5) , with $\boldsymbol{K}_1(\boldsymbol{x}_d) = \boldsymbol{S}_g(\boldsymbol{x}_d) + \boldsymbol{S}_p(\boldsymbol{x}_d)$, $\boldsymbol{K}_2(\boldsymbol{x}_d) = \boldsymbol{P}(\boldsymbol{q}_d)\boldsymbol{T}_f(\boldsymbol{x}_d)\boldsymbol{P}^T(\boldsymbol{q}_d)$, and $\boldsymbol{K}_q = \boldsymbol{P}(\boldsymbol{q}_d)\boldsymbol{K}_{qs}^h\boldsymbol{P}^T(\boldsymbol{q}_d)$ the controller stiffness that has been transformed to joint coordinates. With this interpretation the

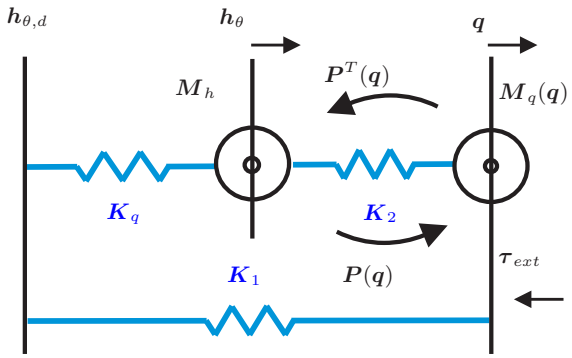

Fig. 5. Visualization of the stiffness components of the stiffness matrix $\boldsymbol{K}$ (cf. equation (31)).

effective joint stiffness $\boldsymbol{K}_{eq}$ can be calculated as

$$\boldsymbol{K}_{eq} = \boldsymbol{K}_1 + (\boldsymbol{K}_2^{-1} + \boldsymbol{K}_q^{-1})^{-1}. \tag{32}$$

The controller stiffness for a given desired effective stiffness can then be formulated as

$$\boldsymbol{K}_q = ((\boldsymbol{K}_{eq} - \boldsymbol{K}_1)^{-1} - \boldsymbol{K}_2^{-1})^{-1}. \tag{33}$$

Thus $\boldsymbol{K}_q$ is specified by the effective joint stiffness. Note that the choice of $\boldsymbol{K}_{eq,d}$ is not trivial since it must be realizable by a positive definite matrix $\boldsymbol{K}_q$. The gains for $\boldsymbol{K}_s$ still need to be chosen in (25). The choice of $\boldsymbol{K}_s$ only influences the joint motion at high frequencies. In general, $\boldsymbol{K}_s$ has to be set as high as it is allowed by the technological constraints (e. g. sample time, sensor resolution, etc.), since the mechanical stiffness of the system has to be maintained, respectively the pulling constraint must be fulfilled. For tendons without tension the equations of motion are no longer valid since the coupling matrix changes structurally. Furthermore, there is a possibility of loss of tendon routing and failure of the mechanism.

[6]The matrices $\boldsymbol{S}_g, \boldsymbol{S}_p$ are symmetric, but, in general, not positive definite.

G. Damping Design

In equation (31), the controller damping $\boldsymbol{D}_{\bar{q}\bar{s}}$ appears only in the equations related to the tendon states $\Delta\boldsymbol{e}_h, \Delta\dot{\boldsymbol{e}}_h$. One possible choice is to define $\boldsymbol{D}_{\bar{q}\bar{s}}$ as a function of $\boldsymbol{M}_{h,d}$ and $\boldsymbol{K}_{\bar{q}\bar{s}}$ with the use of a double diagonalization [18]. The term $\xi \in [0, 1]$, that is obtained by the double diagonalization, represents the damping coefficient and parameterizes the damping term. However, with this damping design the link-side inertia, the stiffness of the tendon network, and the stiffness due to gravity are neglected. Therefore, we propose to use the effective joint stiffness $\boldsymbol{K}_{eq}$ from equation (32) together with the stiffness $\boldsymbol{K}_s$, and to combine it with an effective inertia matrix on task level $\boldsymbol{M}_{eqs}(\boldsymbol{q}_d)$. In order to derive $\boldsymbol{M}_{eqs}(\boldsymbol{q}_d)$ we assume quasi-static conditions such that we can add the task inertia to the tendon inertia $\boldsymbol{M}_{h,d}$. First, $\boldsymbol{M}_{h,d}$ has to be transformed to task coordinates. Using the mapping from equation (22), the tendon inertia represented in task coordinates is given as $\boldsymbol{Q}^T(\boldsymbol{q}_d)\boldsymbol{M}_{h,d}\boldsymbol{Q}(\boldsymbol{q}_d)$. The effective inertia matrix on task level is the sum of the inertia matrices, i.e.

$$\boldsymbol{M}_{eqs}(\boldsymbol{q}_d) = \begin{bmatrix} \boldsymbol{M}(\boldsymbol{q}_d) & \boldsymbol{0} \\ \boldsymbol{0} & \boldsymbol{0} \end{bmatrix} + \boldsymbol{Q}(\boldsymbol{q}_d)^T\boldsymbol{M}_{h,d}\boldsymbol{Q}(\boldsymbol{q}_d).$$

Applying the double diagonalization damping design to $\boldsymbol{M}_{eqs}(\boldsymbol{q}_d)$ and $\boldsymbol{K}_{eqs} = \begin{bmatrix} \boldsymbol{K}_{eq} & \boldsymbol{0} \\ \boldsymbol{0} & \boldsymbol{K_s} \end{bmatrix}$, $\boldsymbol{D}_{\bar{q}\bar{s}}$ is obtained and inserted in equation (25) that is used in the control law (24).

Note that only the use of a full-state feedback control law (e. g. with the state vector $\boldsymbol{z} = (\boldsymbol{h}_\theta, \dot{\boldsymbol{h}}_\theta, \boldsymbol{q}, \dot{\boldsymbol{q}})$) will enable us to specify the complete system behavior using e. g. pole placement techniques. This would represent an extension of the work of Albu-Schäffer [8], [9] and is subject of current research.

V. Simulation: Application to an Antagonistic Finger

The proposed control law is applied to a prototype of a bio-inspired finger prototype (cf. Fig. 6) and evaluated by means of simulations. The finger has four joints driven by eight tendons. The two base joints are realized by a hyperboloid joint that is connected with four tendons. Details on the finger design can be found in [2]. The specific coupling impedes an independent setting of the mechanical stiffness along the q_1- and q_2-axis. According to equation (14), a mechanism with four DOF and 8 tendons related to joint motion has four DOF remaining for the stiffness vector. Since the stiffness components s_{11} and s_{22} turn out to be linear dependent we redefine the stiffness vector introduced in equation (11) to $\mathrm{sv}\{\boldsymbol{S}\} = (s_{11}, s_{12}, s_{33}, s_{44})$.

The controller is evaluated by commanding a step response in the desired stiffness and position. Furthermore, the setting of the effective stiffness is verified by applying a step in the external torque $\boldsymbol{\tau}_{ext}$. In Table II the controller parameters are given. According to Section IV-F the effective stiffness was chosen such that a positive definite $\boldsymbol{K}_q$ was obtained.

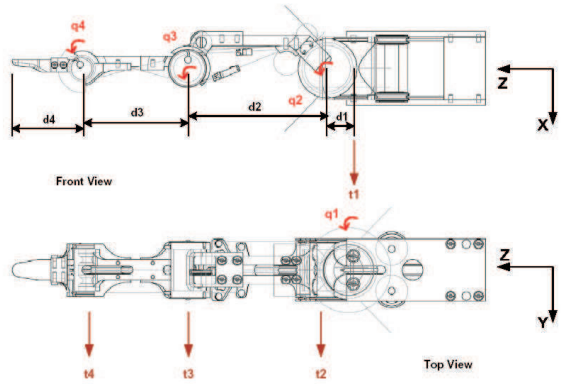

Fig. 6. The index finger prototype of the DLR hand arm system with definition of joint coordinates.

$\boldsymbol{K}_{eq,d}[Nm/rad]$	$\boldsymbol{K}_s[Nm/rad]$
$= \begin{bmatrix} 0.8 & 0.0 & 0.0 & 0.0 \\ 0.0 & 8.0 & -0.06 & 0.8 \\ 0.0 & -0.06 & 2.5 & -1.1 \\ 0.0 & 0.8 & -1.1 & 1.0 \end{bmatrix}$	$= \mathrm{diag}\{25, 25, 25, 25\}$
$\mathrm{sv}\{\boldsymbol{s}_d\}[Nm/rad]$	ξ
$= [30, 0, 10.5, 4.5]$	$= 1$

TABLE II
CONTROLLER PARAMETERS.

In Figure 7 the response of $\boldsymbol{S}$ to a step command in the desired passive stiffness $\boldsymbol{S}_d$ with $\boldsymbol{q}_d = \boldsymbol{0}$ is presented. After 7 ms the mechanical stiffness converges to the new steady-state.

In Figure 8 and 9 the responses of $\boldsymbol{q}$ and $\boldsymbol{h}_\theta$ to a step command of 0.2 rad in $\boldsymbol{q}_{d,2}$ is presented. An overshoot of 0.04 rad can be observed for joint 2 due to the large step size. The strong coupling of the joints 2, 3, and 4 can be observed by the transient behavior of $\boldsymbol{q}_3, \boldsymbol{q}_4$. Joint 1 is not coupled with the other joints and remains undisturbed. After 50 ms the joint positions converge to the desired value. The response of $\boldsymbol{h}_\theta$ (Fig. 9) shows a similar transient behavior. However, it can be seen that $\boldsymbol{h}_\theta$ has a shorter response time than $\boldsymbol{q}$ and converges after 30 ms. Note that from this figure it is difficult to relate the tendon motion to the joint motion and stiffness giving more motivation to our coordinate transformation.

The resulting effect of a step in the external torque $\boldsymbol{\tau}_{ext} = [0.1, 0.1, 0.0, 0.0]^T$ Nm proves the ability to set the effective stiffness $\boldsymbol{K}_{eq,d}$ (cf. Fig. 10). For the same load, q_1 is elongated much more than q_2. The joints q_3, q_4 are also elongated due to their desired coupling with q_2. Since the external torque changes the tendon stiffness the effective stiffness differs from the desired one. For the given load $\boldsymbol{\tau}_{ext}$ the error in the effective stiffness $\boldsymbol{K}_{eq,d}$ is

$$\boldsymbol{K}_{eq,d} - \boldsymbol{K}_{eq} = 10^{-3} \begin{bmatrix} -0.392 & -0.541 & -0.149 & -0.017 \\ -0.541 & -5.129 & -0.076 & 0.131 \\ -0.149 & -0.076 & 0.019 & -0.064 \\ -0.017 & 0.131 & -0.064 & 0.171 \end{bmatrix} \frac{Nm}{rad}.$$

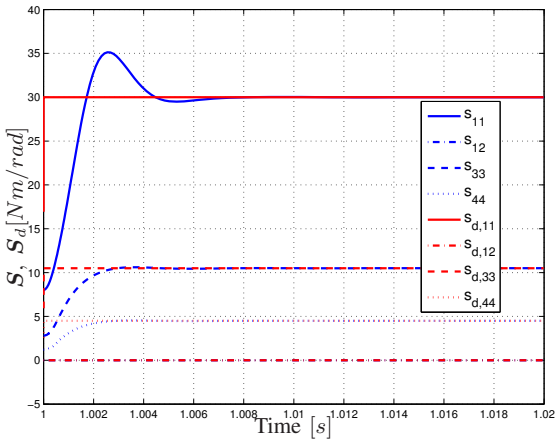

Fig. 7. Response of $\boldsymbol{S}$ to a step in the desired passive stiffness $\boldsymbol{S}_d$. Note that instead of s_{22} the coupling stiffness s_{12} is controlled since s_{11} and s_{22} are linear dependent.

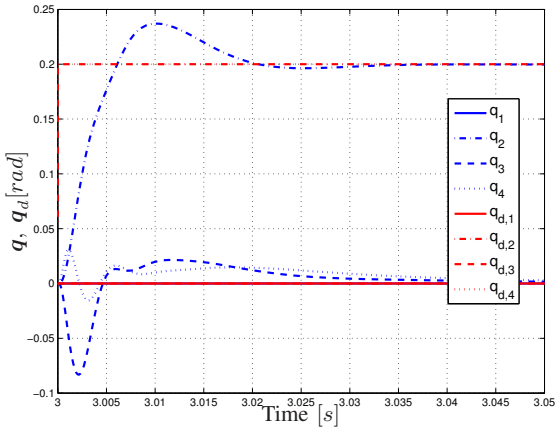

Fig. 8. Response of $\boldsymbol{q}$ to a step in the desired position $\boldsymbol{q}_d$.

Even though in a hyberboloid joint the mechanical stiffness of axis 1 and 2 cannot be set independently using the proposed control laws the desired effective stiffness could be achieved in an excellent manner. The independent setting of the stiffness in the base joint enables us to define a Cartesian stiffness at the fingertip.

VI. CONCLUSION

In this paper, an impedance controller for a tendon-driven mechanism was presented that takes into account both the variable mechanical stiffness and the actively controlled stiffness. This enables us to increase the adjustable stiffness range compared to only specifying a mechanical stiffness. Therefore, desired tendon positions were calculated as a function of the desired joint positions and stiffness exploiting the properties of the exponential force characteristics. These values were used as setpoints in the impedance controller that does not require the properties of an exponential tendon stiffness. Using a transformation matrix that relates the tendon

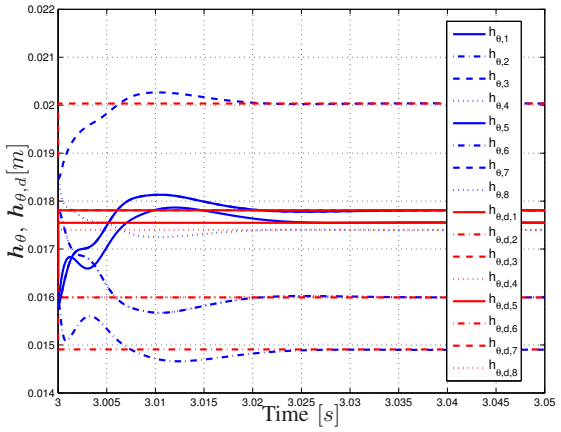

Fig. 9. Response of $\boldsymbol{h}_\theta$ to a step in the desired motor positions $\boldsymbol{h}_{\theta,d}$.

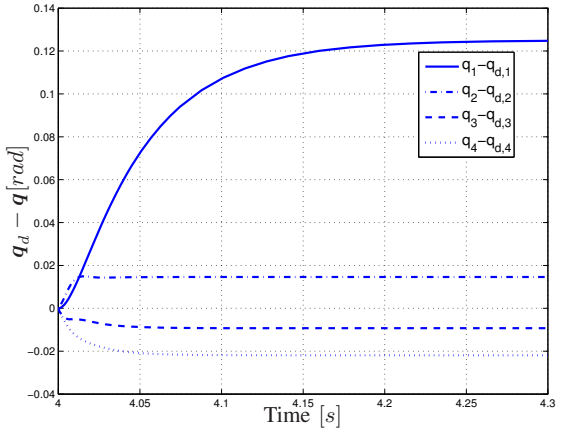

Fig. 10. Response of $\boldsymbol{q}_d - \boldsymbol{q}$ to a step in the external torque $\boldsymbol{\tau}_{ext} = [0.1, 0.1, 0.0, 0.0]^T$ Nm.

position error to joint position and stiffness errors, we could give the mechanism locally a desired effective stiffness. The damping is calculated as a function of the effective mass and effective stiffness of the complete mechanism. In simulation studies we demonstrate the performance by applying steps in the desired position and mechanical stiffness. The reaction to a step in the external torque shows that we can set the desired effective stiffness even for the two axes of a hyperboloid joint.

It is planned to apply the proposed control law to the finger prototype [2]. In future, we will analyze the passivity properties of the proposed controller.

References

[1] J. Butterfaß, M. Grebenstein, H. Liu, and G. Hirzinger, "DLR-Hand II: Next generation of a dextrous robot hand," in *IEEE International Conference on Robotics and Automation*, 2001, pp. 109–114.

[2] M. Grebenstein and P. van der Smagt, "Antagonism for highly anthropomorphic hand-arm system," *Advanced Robotics*, vol. 22, pp. 39–55, 2008.

[3] K. Tahara, Z.-W. Luo, R. Ozawa, J.-H. Bae, and S. Arimoto, "Bio-mimetic study on pinching motions of a dual-finger model with synergistic actuation of antagonist muscles," in *IEEE International Conference on Robotics and Automation*, 2006, pp. 994–999.

[4] A. Bicchi and D. Prattichizzo, "Analysis and optimization of tendinous actuation for biomorphically designed robotic systems," *Robotica*, vol. 18, pp. 23–31, 2000.

[5] H. Kobayashi and R. Ozawa, "Adaptive neural network control of tendon-driven mechanisms with elastic tendons," *Automatica*, vol. 39, pp. 1509–1519, 2003.

[6] G. Palli, C. Melchiorri, T. Wimböck, M. Grebenstein, and G. Hirzinger, "Feedback linearization and simultaneous stiffness-position control of robots with antagonistic actuated joints," in *IEEE International Conference on Robotics and Automation*, 2007, pp. 4367–4372.

[7] G. Palli, "Model and control of tendon actuated robots," Ph.D. dissertation, DEIS, University of Bologna, 2007.

[8] Ch. Ott, A. Albu-Schäffer, A. Kugi, and G. Hirzinger, "On the passivity based impedance control of flexible joint robots," *IEEE Transactions on Robotics*, vol. 24, no. 2, pp. 416–429, April 2008.

[9] A. Albu-Schäffer, Ch. Ott, and G. Hirzinger, "A unified passivity based control framework for position, torque and impedance control of flexible joint robots," *International Journal of Robotics Research*, vol. 26, no. 1, pp. 23 – 39, January 2007.

[10] K. Laurin-Kovitz, J. E. Colgate, and S. D. R. Carnes, "Design of programmable passive impedance," in *IEEE International Conference on Robotics and Automation*, 1991, pp. 1476–1481.

[11] R. Murray, Z. Li, and S. Sastry, *A Mathematical Introduction to Robotic Manipulation*. CRC Press, 1994.

[12] H. Kobayashi, K. Hyodo, and D. Ogane, "On tendon-driven robotic mechanisms with redundant tendons," *The International Journal of Robotics Research*, vol. 17, no. 4, pp. 561–571, 1998.

[13] G. Tonietti, R. Schiavi, and A. Bicchi, "Design and control of a variable stiffness actuator for safe and fast physical human/robot interaction," in *IEEE International Conference on Robotics and Automation*, 2005, pp. 528–533.

[14] A. Albu-Schäffer, M. Fischer, G. Schreiber, F. Schoeppe, and G. Hirzinger, "Soft robotics: What cartesian stiffness can we obtain with passively compliant, uncoupled joints?" in *IEEE/RSJ International Conference on Intelligent Robots and Systems*, 2004, pp. 3295–3301.

[15] P. Tomei, "A simple PD controller for robots with elastic joints," *IEEE Transactions on Automatic Control*, vol. 35, pp. 1208–1213, 1991.

[16] Ch. Ott, *Cartesian Impedance Control of Redundant and Flexible-Joint Robots*. Springer Tracts in Advanced Robotics (STAR), 2008, vol. 49.

[17] J. Baillieul, "Kinematic programming alternatives for redundant manipulators," in *IEEE International Conference on Robotics and Automation*, 1985, pp. 722–728.

[18] A. Albu-Schäffer, Ch. Ott, U. Frese, and G. Hirzinger, "Cartesian impedance control of redundant robots: Recent results with the DLR-light-weight-arms," in *IEEE International Conference on Robotics and Automation*, 2003, pp. 3704–3709.

Appendix

Symmetry of the expression $\frac{\partial \boldsymbol{P}(\boldsymbol{q})}{\partial \boldsymbol{q}} \boldsymbol{f}_t(\boldsymbol{q}, \boldsymbol{h}_\theta)$:

$$\boldsymbol{P}(\boldsymbol{q}) = \left(\frac{\partial \boldsymbol{h}(\boldsymbol{q})}{\partial \boldsymbol{q}}\right)^T = \begin{bmatrix} \frac{\partial h_1(\boldsymbol{q})}{\partial q_1} & \cdots & \frac{\partial h_1(\boldsymbol{q})}{\partial q_n} \\ \vdots & \ddots & \vdots \\ \frac{\partial h_m(\boldsymbol{q})}{\partial q_1} & \cdots & \frac{\partial h_m(\boldsymbol{q})}{\partial q_n} \end{bmatrix}^T$$

$$\begin{aligned} \left[\frac{\partial}{\partial \boldsymbol{q}} \boldsymbol{P}(\boldsymbol{q}) \boldsymbol{f}_t(\boldsymbol{q}, \boldsymbol{h}_\theta)\right]_{k,j} &= \sum_{i=1}^{m} \left(\frac{\partial^2 h_i(\boldsymbol{q})}{\partial q_k \partial q_j}\right) f_i \\ &= \sum_{i=1}^{m} \left(\frac{\partial^2 h_i(\boldsymbol{q})}{\partial q_j \partial q_k}\right) f_i \end{aligned}$$

It can be immediately seen that interchanging the indices k, j yields the same expression and henceforth the symmetry of $\frac{\partial \boldsymbol{P}(\boldsymbol{q})}{\partial \boldsymbol{q}} \boldsymbol{f}_t(\boldsymbol{q}, \boldsymbol{h}_\theta)$ is shown.